Rev. Roum. Sci. Techn.– Électrotechn. et Énerg.
Vol. 63, 1, pp. 19–26, Bucarest, 2018

Dedicated to the memory of Academician Andrei Ţugulea

DIMENSION IMPROVING OF THE LOW VOLTAGE CONTACTOR

ALEXANDRU RADULIAN[1], NICOLAE MOCIOI[1], VIOLETA TSAKIRIS[2]

Key words: Vacuum, Chopping current, Dc actuator, Efficiency, Compactness, Reliability.

Nowadays, contactors, that use ultra-high vacuum technology, have become a viable alternative for the classic air contactors. They are used in order to increase the lifetime in harsh environments, to protect the environment, to reduce costs and the overall dimensions. This article presents the main technical aspects of designing the vacuum contactor according to the latest edition of International Electric Commission standard (IEC 60947). This research was carried out for four years in order to minimize the volume of the vacuum contactor and to increase the technical and the economical performance. The results of the main tests (mechanical endurance, chopping current, breaking capacity, thermal stability) are presented within this article.

1. INTRODUCTION

For ac air-break contactors, commonly used for starting and control applications for power motors, when the circuit is interrupted, the electric arc which occurs between contacts is extinguished outdoors, in free air. In contrast, the vacuum contactor has the electrical contacts embedded in a vacuum chamber, an ideal environment for the arcing, thus achieving the isolation of environment and allowing it to operate in hard conditions of exploitation and harsh working regimes.

Vacuum contactors are utilized as switching or circuit-breaking mechanisms for a variety of alternating current (ac) loads such as: three-phase motors, transformers, surge suppression circuits, capacitors banks and resistive heating loads.

The principle of using ultra-high vacuum in vacuum interrupters includes two basic ideas, namely: increased dielectric rigidity at extremely reduced distances between contacts and the development of the electric arc only in metallic vapors that result from the contacts material. These vapors are condensing very quickly on the cold surfaces of the interrupter, so the vacuum is recovered. Therefore, all vacuum switching devices tend to chopp the current before the natural crossing through the zero moment. The size of the chopping current (which must be max. 5 A) is a quality criterion for the apparatus. The high values of the chopping current together with the inductive component of the circuit lead to the occurrence of the switching overvoltages in the circuit. Thus, in the vacuum switching apparatus, in addition to the normal conditions that a contact must meet, it is required that for a small energy of the electric arc, a sufficient amount of metallic vapors should be developed in order to avoid the early chopping of the current. Given the high dielectric rigidity of the vacuum, the contact stroke can be made very small 2–80 mm, depending on the rated voltage of the apparatus 1–145 kV. Therefore the intensity of the electric field between the open contacts reaches high values and as a result form, dimensions and contact materials are of particular importance. The development of the switching devices with the extinguishing of the electric arc in ultra-high vacuum was made possible by technological advances in two directions, namely the making of metal-ceramic brazing and the obtaining of materials compatible with the ultra-high vacuum, including the materials for electrical contacts. All these technological inovations have led to the development of vacuum interrupters with a reduced volume, much smaller than those in the air, implicitly decreasing the contactor sizes.

Table 1

Comparison of the main manufacturers of low voltage vacuum contactors

Producer	TOSHIBA	TAVRIDA	SIEMENS		EATON-MOELLER	
Model	HCV-1JBU	LSM/TEL1-4/400	3RT12	3TF6	DILM580	DILM 650
RATED VOLTAGE [V]	1500	1000	400		1000	
RATED CURRENT [A]	600	400	400	630	580	650
RATED MAKING CAPACITY [kA]	6	4	4	6.3	5.8	6.5
RATED BREAKING CAPACITY [kA]	4.8	4	3.2	5	4.6	5.2
MECHANICAL LIFE [x 10^6]	2.5	2	10	5	5	
ELECTRICAL LIFE [x 10^6]	0.5	2	1.5		1.2	
SWITCHING FREQUENCY [op./hour]	1200	600	750		1000	
OVERALL DIMENSIONS [mm]	450x348x245	333x190x250	210x 145x 206	232x 230x 237	296x250x232	
VOLUME [dm^3]	38.37	15.82	6.27	12.7	17.17	
WEIGHT [kg]	27	10	9.6	19.5	15	

Table 1 lists the main manufacturers of low voltage vacuum contactors with the parameters provided by each. There is a very large diversity, from manufacturer to manufacturer, of volumes and masses of contactors, for the same parameters.

For example, for the contactor with rated voltage of 400 V and rated current of 630 A, we have:

– TOSHIBA: 38.37 dm^3 – 27 kg
– JOSLYN CLARK: 11.59 dm^3 – 12.7 kg
– SIEMENS: 12.65 dm^3 – 19.5 kg
– Eaton-MOELLER: 17,17 dm^3 – 15 kg.

Maintaining the tendency to reduce the size and weights of the contactors, it is desired to carry out a 400 V/630 A vacuum contactor with a volume less than 11.59 dm^3 and a weight of less than 12.7 kg , having the Eaton-MOELLER contactor as standard .

2. VACUUM INTERRUPTER DESIGN

It is well known that, for electrical contacts used in vacuum contactors, certain requirements need to be met, such as: low chopping current, increased making and breaking capacity, resistance to arc erosion, low tendency to welding, high thermal and electrical conductivity. Features that are dependent on the alloy and method of electrical contacts

[1] ICPE, Splaiul Unirii 313, 030138 Bucureşti, Romania, Email: alex.radulian@icpe.ro
[2] National Institute for Research and Development in Electrical Engineering ICPE-CA, Splaiul Unirii 313, 030138 Bucureşti, Romania

manufacturing and can only be accomplished if the contact material has a fine grain and homogeneous microstructure [1–4]. When disconnecting inductive circuits at currents below 100 A, due to fast diffusion of metal steam into vacuum interrupter, the arc is extinguished before current zero, leading to appearance of pulling power and switching overvoltage. Experimentaly was found that a value of the chopping current less than 5 A, does not affect the electrical network insulation by producing overvoltages [5].

In order to achieve contact pieces for low voltage contacts with vacuum switching at nominal currents of 200 A, 315 A, 400 A and 630 A, needed to replace the classic electromagnetic contactors with air commutation, several techniques were tested. The most significant results were obtained by using two experimental techniques: infiltration and spark plasma sintering.

Infiltration technique was used in order to develop a pair of electrical contacts with 17 mm diameter and 4 mm height. These contacts are developed for the construction of vacuum interrupters, for contactors with rated current of 200–400 A. This contact alloys were made from the following combinations [6]: W-Cu-Ni-Ag (1.6 % Cu, 16.6...19.7 % Ag, 0.8 % Ni and remainder W or 10 % Cu, 9 % Ag, 1 % Ni and remainder W); W-Cu-Ni (18 % Cu, 1 % Ni and remainder W) and W-Cu (26 % Cu, and remainder W) respectively, obtained by sintering-infiltration of the skeletons of W-Cu-Ni (97–2–1) and W–Cu (90–10) respectively, by sheets of Cu, Ag or CuAg50 in liquid phase. The sintering-infiltration process took place in a furnace at a temperature range of 1100–1150 ^{o}C and a dwell time of 30 minutes. These contact pieces had the following characteristics: relative density: between 95.25 and 96.83 %; structural homogeneity as shown in Fig. 1 [6, 7] and low porosity: between 3.17and 4.75 %; electrical resistivity: bewtween 3.12 and 6.15 μΩ · cm; Vickers microhardness HV0.3 / 15 between 212.7 and 260.9.

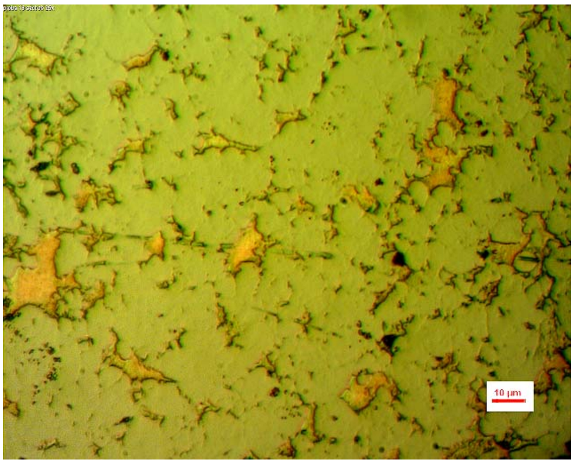

Fig. 1 – Optical microscope image of the W-Cu sintered and Ag infiltrated electrical contact (un-etched state) [6, 7].

Another pair of electrical contact with a diameter of 30 mm diameter and 3 mm heigh was developed in order to be integrated in vaccum interrupters for contactors with rated current of 630 A. The infiltration technique was used for the following systems with tungsten carbide (WC) skeleton [8]: WC-Co-(Cu)-Ag si WC-Cu-Ni-Ag, with 40 %Ag and small additions (0.5–1 %) of alloying elements: Co, Ni and Cu. The skeletons WC-Co-(Cu)-Ag and WC-Cu-Ni-Ag had been infiltrated by Ag tablets in two steps: at 850 ^{o}C and at 1150 ^{o}C. The WC-1% Cu-0.5% Ni-40% Ag composition have been selected for the development of the prototype of electrical contacts able to interrupt currents of 630 A. The following physical-technical properties were obtained: relative density: 97 %; structural homogeneity shown in Fig. 2 [8] and low residual porosity (3 %); Vickers Hardness (HV 285.5); Young Module 135 GPa; electrical conductivity: 24.5 m /Ω · mm^2.

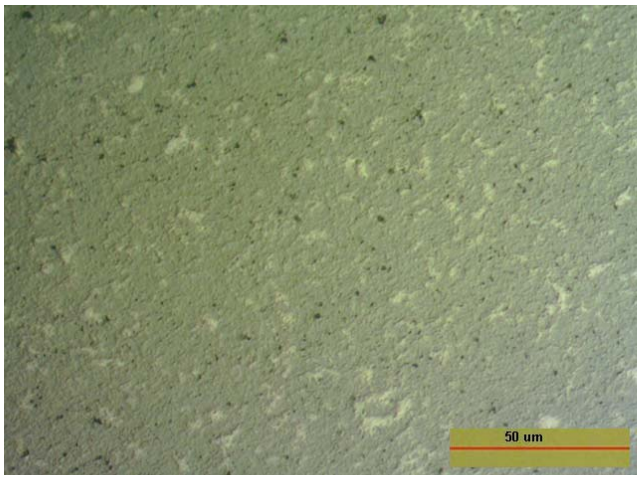

Fig. 2 –Optical microscope image of the WC-1 % Cu-0,5 % Ni-40 % Ag pre-sintered at 850 ^{o}C/30 min and sintered at 1150 ^{o}C/30 min and Ag infiltrated electrical contact (un-etched state) [8].

Spark plasma sintering technique was used in order to develop a pair of electrical contacts with 20 mm diameter and 5 mm height. These contacts are developed for the construction of vacuum interrupters, for contactors with rated current of 200–400 A.This contact alloys were made from the following combinations [9]: W-Cu (30...40 % Cu, remainder W), W-Ag (30...40% Ag, remainder W), W-Cu-Ni (12...14% Cu, 1...3% Ni, remainder W), WC-Cu (30...40% Cu, remainder WC), WC-Ag (30...40 % Ag, remainder WC and WC-Co-Ag (0.5...5 % Co, 40 % Ag, remainder WC. The contact materials were prepared by powder metallurgy method: powders mixing-simple homogenization in an automatic device/mechanical alloying in a planetary mill for 10 hours-spark plasma sintering in vacuum in the temperature interval: 900–1 200 ^{o}C.

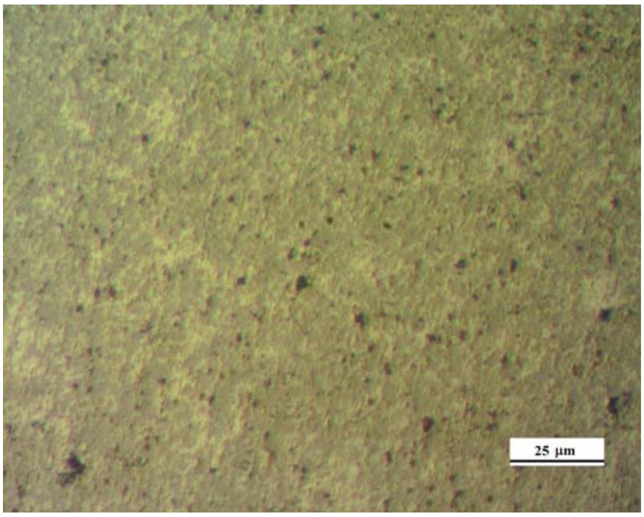

Fig. 3 – Optical microscope image of the WC–40 % Ag–0.5 % Co sintered by SPS at 925^{o}C/5 min (un-etched state) [9].

The contact material was prepared by simple homogenizing of elemental powders in a Turbula type mixer for 5 h, followed by sintering of the homogeneous powder mixture by spark plasma sintering (SPS) at temperature of 900–930 °C and dwell time of 5 minutes.The physical-technical and functional characteristics of the WC-40 % Ag-0.5 % Co prototype are the following: relative density: 97.56%; structural homogeneity as shown in Fig. 3 [9] and low residual porosity (2.44 %); Vickers Hardness (HV 207.52); Young Module: 182.068 GPa; electrical conductivity: 21.75 m /$\Omega \cdot mm^2$; average chopped current: 0.39 A; maximum chopped current: 0.75 A. The distribution of the chopping current values for different contact materials is shown in Fig. 4. For each material, at least 31 measurements were carried out in order to obtain accurately values for chopping current and his standard deviation [10].

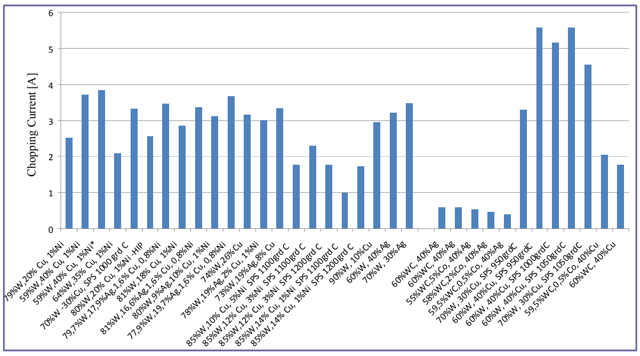

Fig. 4 – Chopping current for different contact materials [10].

The diagram shows that the WC–40 % Ag–0.5 % Co material obtained the lowest value of the chopping current 0.39 A. This contact material was used in the development of the vacuum interrupter. The sketch of the vacuum interrupter is shown in Fig. 5.

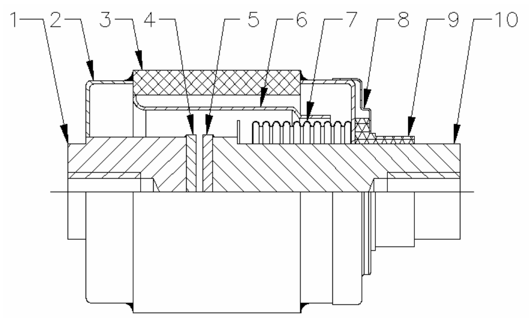

Fig. 5 – Experimental setup for the mechanical endurance test.

The constructive elements of the interrupter are the following: fixed contact rod 1, cover plate 2.8, Al_2O_3 insulator, fixed contact 4, movable contact 5, fixed arc shield 6, bellows 7, guide bush with antitwist 9, movable contact rod. All of these components are made of materials compatible with ultra-high vacuum. The pressure inside the interrupter is 10^{-7}–10^{-8} mbar. Their practical realization was done by means of a vacuum brazing furnace which worked according to a specific temperature-time characteristic. After dielectric strength and rate of loss of vacuum tests, the vacuum interrupters were fixed in the final contactor assembly. Note that the volume of a vacuum contactor is given by the in-line positioning of the vacuum interrupters, the arrangement of the spring system and the size of the electromechanical actuator. In order to limit these inconveniences, we have found the following solution: 1) to arrange the longitudinal axes of the vacuum interrupters in each corner of an equilateral triangle; 2) to locate the opening spring and the electromechanical actuator to be in the axis of the resulting force produced by the antagonistic forces. This has the consequence of reducing the volume and balancing the forces that appears in the kinematic system of the contactor [11].

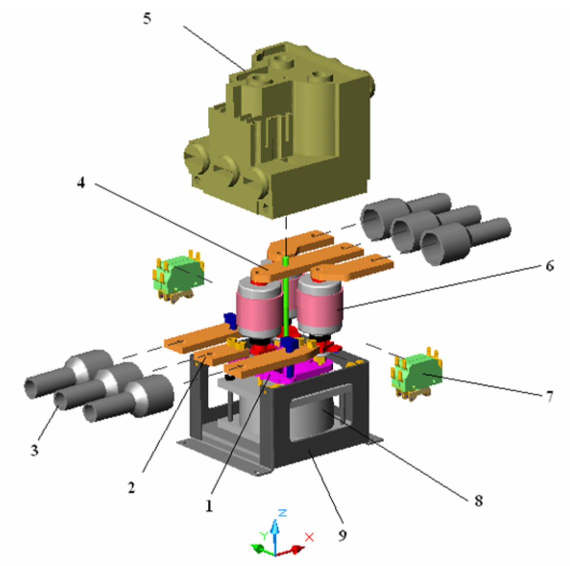

Fig.6 – The structure of the vacuum contactor – CAD version.

Figure 6 shows the structure of the vacuum contactor. The main elements of the contactor are: movable armature 1, lower main conductor terminal 2, protection sleeves 3, upper main conductor terminal 4, resin housing 5, vacuum interrupters 6, auxiliary switches 7, electromagnetic actuator 8, operating mechanism box 9. The role of electrotechnical rubber sleeves 3 is to increase the degree of safety in operation.

Figure 7 shows a longitudinal section of the electromagnetic actuator 8. From a constructive point of view, it is a classic dc plunger electromagnet, made in an axisymmetric construction, whose magnetic circuit is made of low carbon steel.

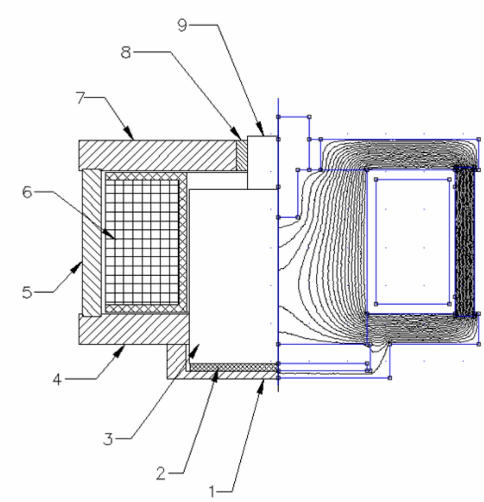

Fig. 7 – Longitudinal section of the electromagnetic actuator: left side – CAD version; right side – FEM version.

The closing and holding forces have been calculated from the sum of the antagonistic forces that are developed by: the opening spring, the contact pressure springs, the flexible conductors, the auxiliary contacts and the mass of the moving part. Thus, the sum of the resulting antagonistic forces was 940 N and the force obtained from the calculations and simulations was 1 450 N. The force difference is acceptable since the contactor must be able to close at 0.85 of the supply voltage. Note that the holding force in the closed position is achieved when the coil is excited with a current I_H of 0.23 A. In the closing process, the coil is powered by 220 Vdc and absorbs a current I_C of 1.4 A. Switching from 1.4 A to 0.23 A is done by a toroidal transformer that initially feeds the coil from the primary winding and then switches over the secondary winding. Thus, the power consumption in the closed position becomes 8 VA. This solution eliminates the overheating produced by the classical economizer resistors.

3. EXPERIMENTAL RESULTS

3.1 VERIFICATION OF MECHANICAL PERFORMANCE

Verification of the mechanical endurance requires fixing the apparatus to a normal operating position on a rigid metal frame (Fig. 8), which does not oscillate under the action of the contactor operations. The device must carry out the number of operations (without load) provided with its own electromagnetic actuator which is powered at the rated voltage.

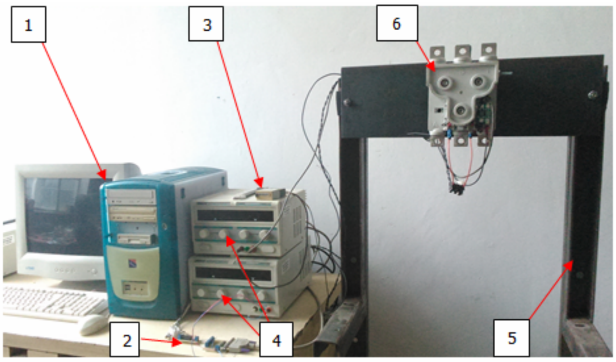

Fig. 8 – Experimental setup for the mechanical endurance test.

The switching frequency must be at least equal to the nominal switching frequency, but for the acceleration of the test it is allowed to perform the test at a higher connection frequency, taking additional measures to cool the coil. The coil can be replaced during the tests. Figure 8 shows the installation used to check the mechanical endurance, which is composed of: 1 – computer, 2 – programmer, 3 – counter, 4 – dc source, 5 – metal frame, 6 – probe contactor. Having the system composed of computer and programmer 2, the probe contactor 6 was able to operate with a connection frequency of 1 800 operations per hour, the number of mechanical maneuvers being recorded with the analog counter 3.

Regarding the lifetime evaluation of the contactor, we can state that the value of the technical solution adopted has been experimentally confirmed by over 2.5 million maneuvers with minimal technical changes, relative to the rigidity of some electronic components and the modification of a bearing.

In order to measure the electromechanical parameters of the vacuum contactor, the measuring stand shown in Fig. 9 was used. From the constructive point of view, the stand is composed of: 1 – Tektronix TDS 5104 digital oscilloscope, 2 – coaxial shunt with Rs = 1.225 mΩ, 3 – Linear Pennygiles SLS095 linear transducer, 4 – dc source and 5 – probe contactor. The waveforms shown in Fig. 10 were captured with the oscilloscope mentioned above. These waveforms also validate the analytical results presented in chapter 3 on the closing and holding currents.

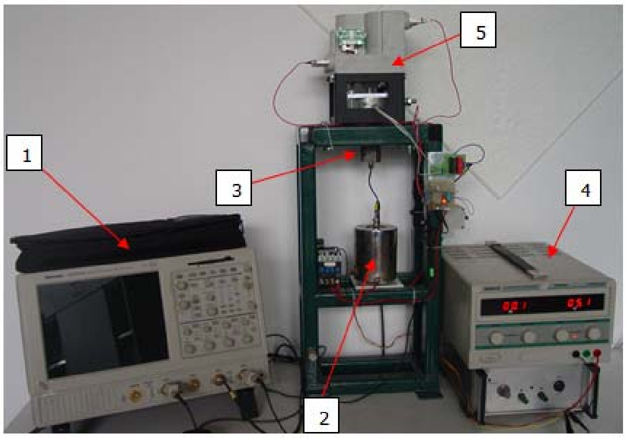

Fig. 9 – Experimental setup for measuring the electromechanical parameters of the contactor.

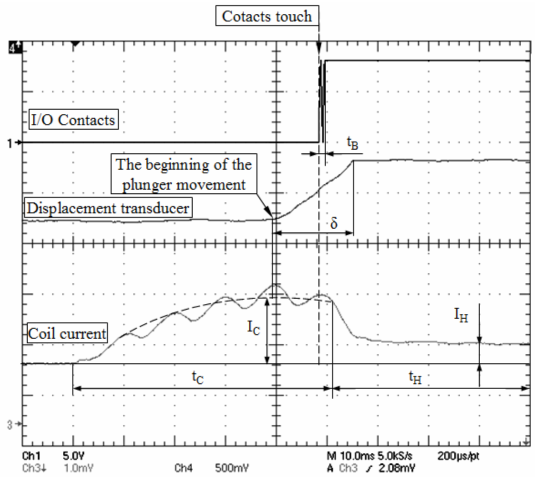

a)

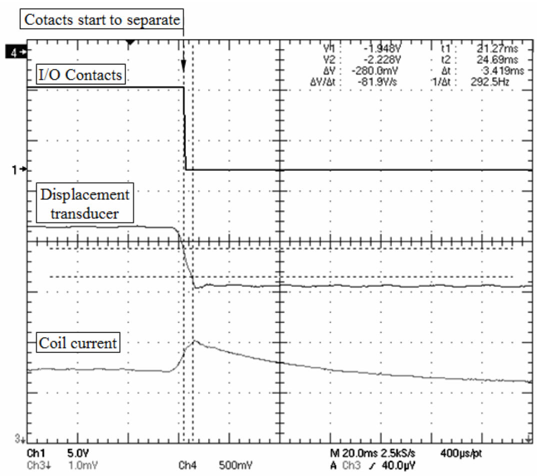

b)

Fig. 10 – The waveforms of the sequences: a) closing; b) opening.

So it is noted from the Fig. 10a that the closing current I_C has a value of 1.42 A for t_C = 52 ms and then passes on the holding current I_H which has the value of 0.24 A during the time t_H. It can be observed that when the contacts touch, due to the hardness of the carbide-based contact alloys, a bouncing ocuurs for t_B = 3 ms. This time can be reduced by reducing the closing speed, but this may cause adverse effects in the switching process. More measurements have been performed to determine precisely the bouncing time t_B for each pole of the contactor. The rated stroke of the electromagnet is $\delta = 5$ mm and the and distance between electrical contacts is $d = 2$ mm. The closing speed measured at last 33 % of rated stroke was v_C= 0.4 m/s. Figure 10b shows the opening oscillogram. The opening speed measured at last 75% of rated stroke was v_O = 0.6 m/s. According to these results we can state that the contactor is in nominal parameters imposed by the standard in force. There must be a very precise correlation between the electromechanical parameters of the actuating system and the parameters of the vacuum interrupters in order to achieve the desired performance.

3.2. VERIFICATION OF ELECTRICAL PERFORMANCE

The heating test was carried out according to the standard in force IEC 60947. The overview of the test circuit for the thermal stability of the contactor is shown in Fig. 11. In principle, the test facility shown in Fig. 11 is composed of: – AT – 75 kVA autotransformer, T – 80 kVA high current transformer, DT – FLUKE 54II digital thermometer with thermocouple, CT – current transformer, A – Digital ammeter, Cx – probe contactor.

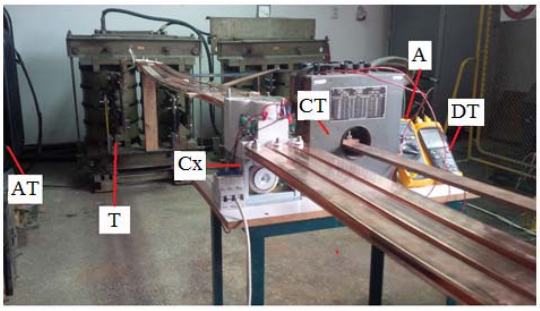

Fig. 11 – Overview of the test circuit at the thermal stability of the contactor.

A current of 400 and 630 A RMS was applied to the contactor for 8 hours, while the contactor reached the stabilized temperature. The temperature at the terminals of the contactor was measured with a digital thermometer and with a thermo-camera type FLIR ThermaCam B640. The ambient temperature was about 20 ± 2^0C. The results are shown in Table 2 and Fig. 12.

Table 2

Heating temperatures recorded during the thermal stability test

Terminal	Current [A]					
	400			630		
	T_t [°C]	T_c [°C]	ε [%]	T_t [°C]	T_c [°C]	ε [%]
L1	43.3	41.3	4.61	61.8	68.8	–10
L2	43.5	42.2	3.08	59.4	70.3	–15
L3	44.8	44.6	0.44	70.7	71.2	–0.7
L4	48.8	47.7	2.3	77.1	83.1	–7.22
L5	43.6	42.6	2.3	70	70.3	–0.42
L6	42.1	42.7	–1.4	65.9	67	–1.64

T_t is the temperature measured with thermocouple [°C] and T_c with the thermal imaging camera [°C].

It can be seen that the temperatures reached are within the limits imposed in the related standard.

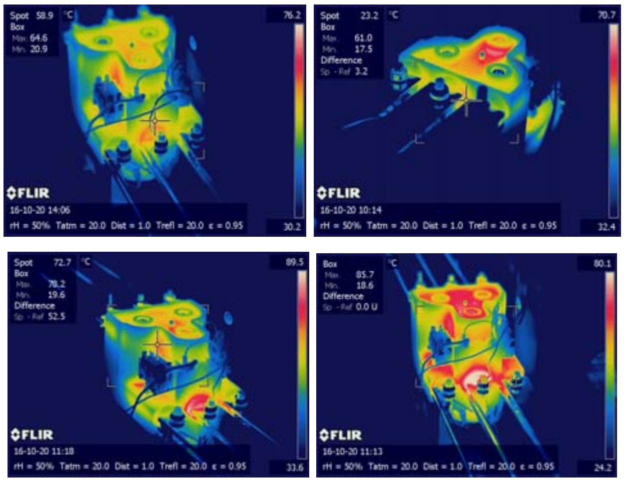

Fig. 12 – Images captured with the thermal imaging camera during the thermal stability test of the contactor.

Breaking capacity represents the RMS value of the interrupted current measured at the separation moment of contact elements and without suffering sensitive damages of the contactor. Breaking capacity is the current that the contactor must disconnect (more than 50 times) and gives an indication of the possibility of interruption of motor starting currents ($I_p \geq 6$ I_n). These currents must be disconnected when the contactor is used in AC4 regime.

For carrying out the breaking tests, it was used the simplified circuit diagram shown in Fig. 13. Abbreviations are described as follows: Q1 – 10 kV vacuum circuit breaker, Q2 – air load switch, T1 – 6.3 MVA, 10/1 kV three phase transformer, Q3 – air load switch, Q4 – 1 kV vacuum circuit breaker, K1 – ultra-fast switch, X – probe contactor, *R* – resistance, *L* – inductance, *C*S – coaxial shunt, VD – voltage divider and OSC – oscilloscope.

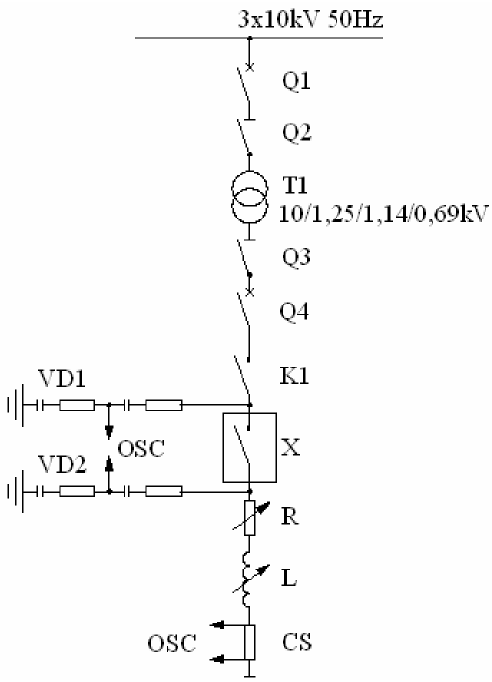

Fig. 13 – Circuit diagram for breaking capacity test.

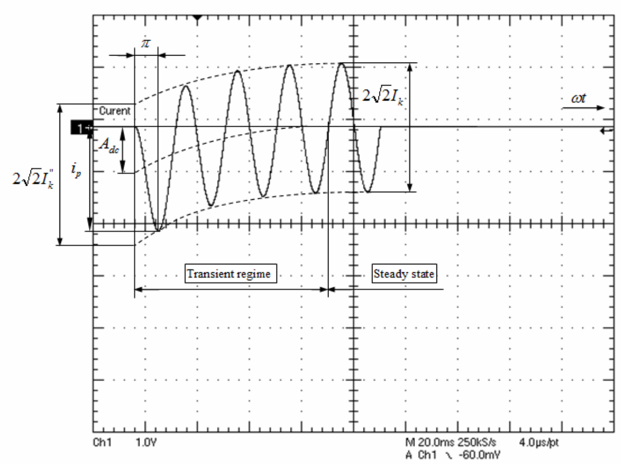

Fig. 14 – Asymmetrical short-circuit current waveform, α = π/2.

Figure 14 shows the waveform of the test current. This oscillogram shows the evolution of the presumed current, which satisfies the relation [5]:

$$i = \hat{I}_k''(\sin\alpha \cdot \mathrm{e}^{-\frac{t}{T}} + \sin(\omega \cdot t - \alpha)), \tag{1}$$

$$T = \frac{L}{R}; \tag{2}$$

$$\alpha = \varphi - \psi, \tag{3}$$

where:

$\hat{I}_k''$ – initial symmetrical short-circuit current;

i_p – peak short-circuit current;

I_k – steady-state short-circuit current;

A_{dc} – initial value of the d.c. component i_{dc};

T – time constant of the circuit;

L – inductance of the circuit;

R – resistance of the circuit;

α – angle between the initiation of the fault and zero voltage;

φ – phase angle (current with respect to voltage);

ψ – circuit connection angle relative to the source voltage.

In the situation α = 0, the presumed current is symmetrical, with the expression [5]:

$$i = \hat{I}_k'' \cdot \sin\omega \cdot t\,. \tag{4}$$

For the value α = π / 2, the presumed current accuses a maximum asymmetry, as follows [5]:

$$i = \hat{I}_k''(\mathrm{e}^{-\frac{t}{T}} - \cos\omega \cdot t)\,. \tag{5}$$

In this case, the aperiodic component takes the form [5]:

$$i_a = \hat{I}_k'' \cdot \mathrm{e}^{-\frac{t}{T}}. \tag{6}$$

The adjustment of the power factor and the current intensity is achieved through the variation of resistance R and inductance L. The opening and closing sequences of electric apparatus have been given using an electronic programmer which, at the same time, has achieved the acquisition of current and voltage signals. Different currents have been applied to each pole of the contactor.

On this basis, as shown in Fig. 14 we can calculate the value of the power factor of the test circuit (cos φ). For the performed tests, the power factor cosφ varies in the domain [0.25 ÷ 0.35]. Thus, switching tests have been carried out on the vacuum interrupters mounted on the contactor mentioned above at the following currents at RMS value: 573 A, 3 600 A, 3 622 A, 3 954 A, 4 080 A, 4 626 A, 5 482 A, 6 000 A. The success rate was 100 %. Due to the absence of an axial or radial magnetic field generator, the breaking current value was limited to 6 000 A, because at this current the arc is diffused. Considering that the contactor is not a protective device and the interrupted currents are not in the tens of kiloamps, as in the case of the circuit breakers, the mounting of magnetic field generators is not technically and economically justified.

Figure 15 shows a typical breaking oscillograms recorded during the tests. It provides information about the evolution of the vacuum arc. The voltage and current wave forms have been acquired by the oscilloscope OSC via coaxial shunt CS and voltage divider VD. It can be observed that the ultra-high vacuum arc has a characteristic shape of voltage, in which lacks the depression between the peaks.

Therefore, for one semiperiod, the arc voltage waveform is described by three parameters: U_k – cathodic voltage, U_m – maxim voltage, U_f – final voltage. This waveform corresponds to a value related to the ωτ (ω – pulsation at 50 Hz and τ – the arc time constant) that is ranging between 0.7 and 1. This proves that the electric arc in vacuum has a relatively low power dissipation compared to the electric arc in air. The value of the final voltage U_f corresponds to the voltage of last cathodic spot, before the arc extinguishes at zero current (z.c.). This value gives a clue of the initial value of the residual electrical conductivity G_0 at z.c.. It can be observed that as the interrupted current increases, the final U_f voltage decreases. This fact proves a dependence between the residual conductivity G_0 and the current. On this basis it was detected the critical value of U_f which compromise the success of the interruption. This critical value of U_f can be associated with a specific type of vacuum interrupter and can serve as quality criteria [12].

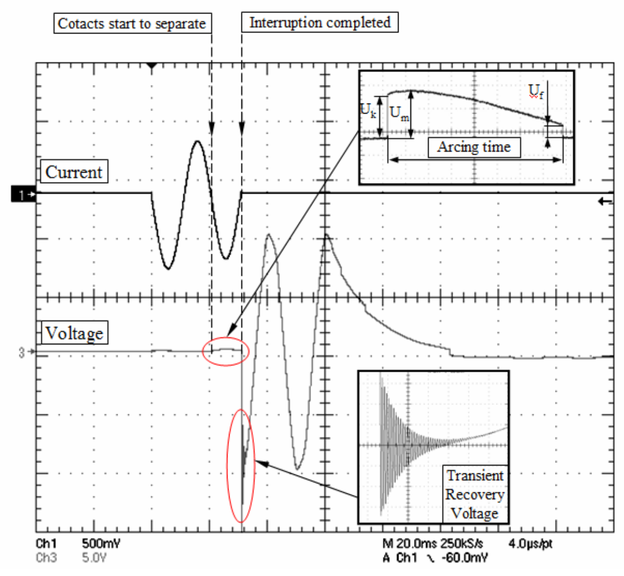

Fig. 15 – The detailed waveform of a sequence of interruptions.

Figure 16 show images of WC-Ag-Co cathode after multiple short-circuit current interruptions.

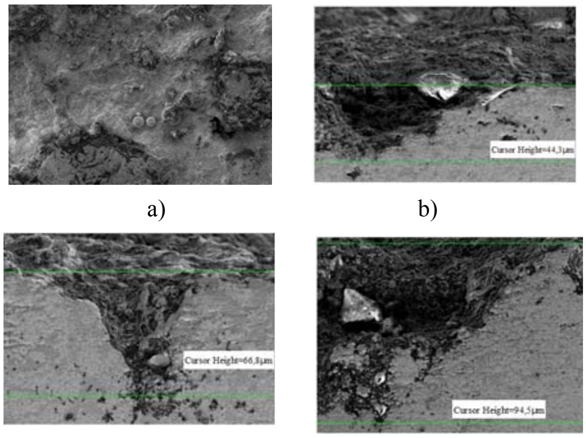

a) b)

c) d)

Fig. 16 – Different images of micro-craters formed during the arcing process in the WC - Ag - Co cathode: a) contact surface; b), c), d) cross section on top of the contact.

The images were captured with scanning electron microscopy (SEM) equipment. Changing the structure of the contact surface and the beta factor leads to the change of the electric field and to the occurrence of the breakdown phenomenona. It is noticed that the erosion is not uniform distributed over the entire surface of the contact, so the heating is not optimal and after several repeated discharges it can destroy the material. These craters become sources of macroparticles of different sizes and shapes which are emitted due to the violent plasma-liquid pool interactions at the cathode spot [13, 14]. After dislocation, the particles tend to migrate into the space between the contacts and some tend to be deposited on cold surfaces. The absence of a magnetic field generator (axial or radial) acting on the plasma makes the arc difficult to control and locate in a position. This control is especially necessary for the vacuum interrupters for circuit breakers where the interrupted current is in the order of tens of kA.

4. CONCLUSIONS

The subject of the article was approached in a scientific manner focusing on the study of elementary and complex phenomena, but also of constructive peculiarities for the same performance of the contactor. In parallel with this research flow, an increased attention has been paid to the optimization of the manufacturing cost of the final result. The use of design environments and computerized simulation have led to a much more accurate approach of the challenges.The experimental results have led to the reduction of physical parameters compared to the Eaton - Moeller reference contactor model, as follows:

– reduced weight by 46 % (8 kg *vs*. 15 kg);

– overall dimensions by 62 % (140 × 210 × 213 *vs*. 250 × 286 × 232).

The prototype of the low voltage vacuum contactor has the following performance (Table 3). The overall picture of the contactor can be seen in Fig. 17

The chosen drive system placed at the center of the reactive forces ensures a balanced stress which leads to a high mechanical lifetime. The small number of parts, as well as their simple assembly technology, increase the reliability of the drive system and reduce the number of maintenance operations in service.

The tests performed according to the international standard on the physical model were made in order to determine the capabilities of the projected apparatus.

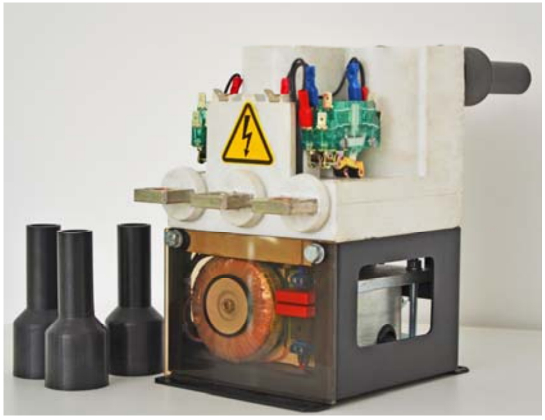

Fig. 17 – The prototype of the low voltage vacuum contactor resulted.

Table 3

The main performance of the resulting contactor

Producer	ICPE
Model	NeWaLC
RATED VOLTAGE [V]	1200
RATED CURRENT [A]	630
RATED MAKING CAPACITY [kA]	6
RATED BREAKING CAPACITY [kA]	6
MECHANICAL LIFE [x 10^6]	2.5
SWITCHING FREQUENCY [op./hour]	1200
OVERALL DIMENSIONS [mm]	140×210×213
VOLUME [dm^3]	6.26
WEIGHT [kg]	8

ACKNOWLEDGMENTS

This work was financially supported by the Executive Agency for Higher Education, Research, Development and Innovation Funding through the Financial Agreement PCCA no. 34/2012.

Received on August 21, 2017

REFERENCES

1. P. Slade, *Electric Contacts for Power Interruption: A Review*, 20th ICEC, 2000, pp. 239–245.
2. Ludwar, W.F. Rieder, Proc. 13th Int. Conf. on Electric Contacts, Lausanne, 1986, p.156.
3. J.C. Kim, I.H. Moon, *Sintering of Nanostructured W-Cu Alloys Prepared by Mechanical Alloying*, J. NanoStructured Materials, **335**, *1–2*, pp. 283–290 (2002).
4. Z. Qiaoxin, S. Xiaoliang, Y. Hua, D. Xinglong, *Microstructure and Properties of W-15Cu Alloys Prepared by Mechanical Alloying and Spark Plasma Sintering Process*, Journal of Wuhan University of Technology-Mater, Sci. Ed., Jun 2008, p. 401.
5. G. Hortopan, *Aparate electrice de comutatie*, Vol. 2, Editura Tehnică, Bucharest, 1996.
6. V. Tsakiris, *Un nou contactor de joasa tensiune, cu comutatie in vid, tip compact* (Contract nr. 34/2012), Raport Faza 1 Partener 3 (ICPE-CA)/2012: Elaborare soluție nouă și realizare model experimental.
7. V. Tsakiris, M. Lungu, E. Enescu, D. Pavelescu, G. Dumitrescu, A. Radulian, V. Braic, *W-Cu composite materials for electrical contacts used in vacuum contactors,* Journal of Optoelectronics and Advanced Materials, **15**, *9–10*, pp. 1090–1094 (2013).

8. V. Tsakiris, *Un nou contactor de joasă tensiune, cu comutație în vid, tip compact* (Contract nr. 34/2012), Raport Faza 5 Partener 3 (ICPE-CA)/ 2016 – Experimentare prototipuri de contactoare cu comutație în vid (final).
9. V. Tsakiris, *Un nou contactor de joasă tensiune, cu comutație în vid, tip compact* (Contract nr. 34/2012), Raport Faza 3 Partener 3 (ICPE-CA)/2014 – Testare modele funcționale (MF), proiectare și realizare prototipuri de contactoare cu comutație în vid.
10. A. Radulian, N. Mocioi, I. Deaconu, *Chopping current phenomena for various contact materials*, Revista EEA, **63**, *4*, 2015.
11. G. Dumitrescu, R. Calistru, D.A. Pavelescu, A. Radulian, *Three-pole vacuum electromagnetic contactor, the compact type*, Patent application nr. A/00176/2013.
12. G. Dumitrescu, A. Radulian, *Un nou contactor de joasă tensiune, cu comutație în vid, tip compact* (Contract nr. 34/2012), Raport Faza 5 Partener 3 (ICPE)/2016 – Experimentare prototipuri de contactoare cu comutație în vid (final).
13. E. Dullni, P. Picot, *Perofrmance of vacuum circuit breakers with contact bouncing during closing*, 21st International Conference on Electricity Distribution, Paper 0439, Frankfurt, 6–9 June 2011.
14. L.A. Garcia, D.E. Rincon, J.R. Yepes, P.J.A. Arango, E.R. Parra, *Metallic cathode surface modification by using low-pressure pulsed vacuum arc discharge*, DYNA (Medellin),**79**, *176*, pp. 90–98 (2012).